

Effect of Ammonium on Anion Uptake and Dielectric Relaxation In Laboratory-Grown Ice Columns

Gerardo Wolfgang Gross* and Robert K. Svec

Department of Environmental and Earth Science, New Mexico Institute of Mining and Technology, Socorro, New Mexico, 87801

Received: October 11, 1996; In Final Form: June 3, 1997[®]

Inorganic acids or their alkali-metal or alkaline-earth salts are rather insoluble in ice. Ammonium ion, however, enhances the uptake of a variety of anions into the ice matrix. In the specific case of the fluoride this has been known for almost 50 years and attributed principally to isomorphism between the NH_4F and ice crystal lattices. We report here that ammonium also enhances the solubility in ice of anions that do not fit easily into the ice structure. With the species pair $\text{HCl}/\text{NH}_4\text{Cl}$ we document specific effects of ammonium on anion uptake, static conductivity, and dielectric conductivity in ice. Other ion species for which comparable results have been obtained are mentioned. Possible implications for atmospheric processes are briefly discussed.

Introduction

Ice is notoriously intolerant of impurities. If grown slowly enough it will almost completely reject inorganic chemical species in the water, and especially the cations. Nonetheless, for close to 50 years it has been known that ammonium *fluoride* can form solid solutions with ice, of up to about 10 wt %, and that electrical response characteristics are profoundly changed from those of ice doped with HF or an alkali metal fluoride.¹ It was reported even earlier that ammonium *chloride* reverses the sign of the freezing potential.² Some of these phenomena could be significant for atmospheric processes (vide infra). This work uses improved methods to continue early investigations extending them to other anions common in the atmospheric environment. For detailed presentation in this paper we have singled out HCl and NH_4Cl because these species are of substantial environmental interest and their effects on ice are typical for the investigated solutes.

Methods

A. Solute Uptake—Distribution Coefficient. Ice columns ($l = 20\text{--}25\text{ cm}$, $\phi = 3.8\text{ cm}$) were grown from dilute solutions under quasi-equilibrium conditions. The columns were melted and analyzed in 1.5 cm slices. The experimental method is described in detail elsewhere.^{3,4} The initial solute concentrations in the water ranged from 10^{-6} to $10^{-1}\text{ g equiv L}^{-1}$, depending on solute species and the sensitivity of available analysis methods. The upper limit of the concentration range used for a particular solute was determined by the need to avoid or minimize “interface breakdown”⁵ (ref 4, Figure 9). Continuous stirring of the solutions a few centimeters above the interface served this purpose; it also kept solute concentration in the melt nearly uniform, facilitating computations, and it minimized the trapping of liquid droplets in grain boundaries. Chloride solutions were spiked with Cl-36 , bicarbonate solutions with C-14 , and measured by scintillation counting. Other ions were determined by liquid ion chromatography with conductivity suppression.

From the analysis data, the distribution coefficient is computed for each slice interval.⁴ It is defined as

$$k_x = C_s(x)/C_L(x)$$

where $C_s(x)$ = solute concentration on the solid side of an

interface at distance x from the origin of freezing (measured and reported as solute concentration in the melted ice at room temperature) and $C_L(x)$ is the concentration on the liquid side of the same interface. The slowly varying concentrations are averaged over the slice interval.

B. Electrical Measurements. A computer-controlled lock-in amplifier was used to measure the real and imaginary parts of the dielectric relaxation spectrum of selected (unmelted) slices at 31 frequencies in the range 1 Hz to 100 kHz at 13 temperatures between about -1 and $-85\text{ }^\circ\text{C}$. To suppress electrode reaction effects, a thin linear blocking layer^{4,6} is inserted between each electrode and the ice sample creating a layered (Maxwell–Wagner type) capacitor.⁷ The ice parameters are recovered from the layered-capacitor data by computation.⁸ This paper reports primarily on electrical conductivity and its frequency dependence.

Results

Distribution coefficients and conductivity data for ice doped with chloride are shown in Table 1. Data for pure ice and several other anions are shown for comparison.

A. Chloride Uptake in Ice. HCl or alkali metal salt (NaCl , etc.) chloride exhibits a concentration-independent k of $(2\text{--}3) \times 10^{-3}$, while for *ammonium* chloride k is consistently $(9\text{--}12) \times 10^{-3}$ (Table 1; Figure 1).^{4,9,10} For the sulfate and the nitrate the contrast is even larger (Table 1).

B. Electrical Conductivity. Ice samples doped with trace amounts of HCl (or one of its alkali metal salts) and NH_4Cl , respectively, show contrasting features in their electrical conductivity response. This is illustrated with complex conductivity plots¹¹ in Figures 2 and 3, which exhibit the response of samples doped with comparable chloride concentrations.¹² The complex conductivity is

$$\sigma^*(\omega) = \sigma'(\omega) + i\sigma''(\omega) \quad (1)$$

Expressed in terms of the complex dielectric constant, it is

$$\sigma^*(\omega) = \epsilon_0 \left\{ \frac{\sigma_0}{\epsilon_0 + \epsilon''(\omega)\omega} + i\epsilon'(\omega)\omega \right\} \quad (2)$$

where ϵ_0 = permittivity of free space [$8.854 \times 10^{-14}\text{ F cm}^{-1}$] and $\omega = 2\pi f$ (angular frequency). The conductivity is given by the real part of eq 2 and consists of two terms: σ_0 is the frequency-independent, dc or static, conductivity of *free* charge

[®] Abstract published in *Advance ACS Abstracts*, July 1, 1997.

TABLE 1: Sample Data (Conductivities at $-60 \pm 1^\circ\text{C}$)

solute	C_s^a	k_s^b	σ_0^c	$\Delta\sigma_D^c$	σ_∞^c
HCl	0.07	2.6	700	1000	1700
HCl	0.29	2.3	4000	1000	5000
HCl	1.3	2.3	8000	2000	10000
NH ₄ Cl	0.07	10.6	30	970	1000
NH ₄ Cl	0.6	9.0	3	5000	5000
NH ₄ Cl	3.7	6.1	2	10000	10000
H ₂ O	0.0		67	26	93
H ₂ SO ₄	0.014	0.16	16	62	78
H ₂ SO ₄	0.018	1.3	<7	>88	~95
H ₂ SO ₄	0.192	0.22	≤14	≥82	≥96
(NH ₄) ₂ SO ₄	8.16	4.5	<0.1	2800	2800
(NH ₄) ₂ SO ₄	18	2.6	<0.1	3000	3000
KNO ₃	0.014	0.23	570	30	600
KNO ₃	0.040	0.17	1250	250	1500
KNO ₃	0.20	0.17	1700	3300	5000
NH ₄ NO ₃	0.012		<0.1	≤180	≤180
NH ₄ NO ₃	0.29	5.4	≤0.3	3800	3800
NH ₄ NO ₃	0.59	5.4	≤0.26	7000	7000
NaHCO ₃	0.005	0.31	<12	48	50
NaHCO ₃	0.01	0.37	<1	42	≤45
NH ₅ CO ₃	0.05	0.4	<23	<73	88
NH ₅ CO ₃	0.5	21	<2	75	~100
KF	0.2	≤81	≤2700	≥3300	6000
NaF	0.5	29	~4000	>1000	5600
NaF	0.95	4.4	≤100	5200	5300
NH ₄ F	0.25	81	<212	≥207	>437
NH ₄ F	133	≤445	<16	~5800	5800

^a ppm anion. ^b $\times 10^{-3}$. ^c $\times 10^{-11} \text{ S cm}^{-1}$.

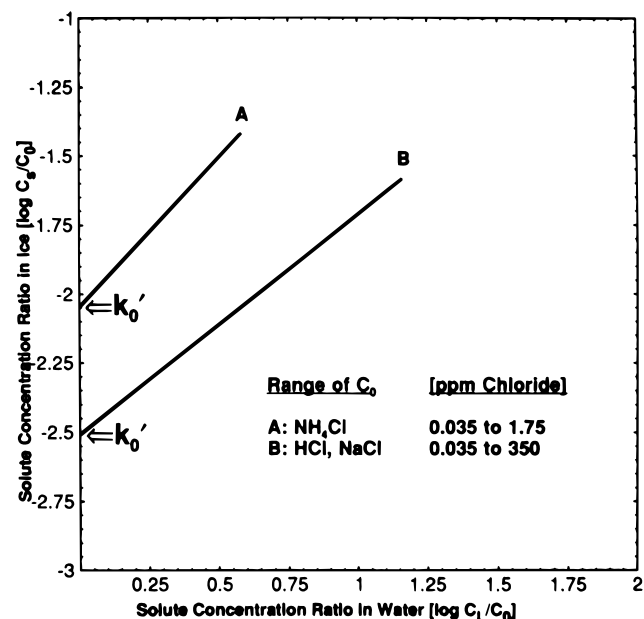


Figure 1. Representative chloride distribution curves. k_0' = distribution coefficient extrapolated to onset of freezing.⁴ C_0 = solute concentration in the melt prior to freezing. For other symbols see text. Distribution curves for HCl and for the alkali-metal chlorides are identical to second-order or better.⁴

(conduction current); $\epsilon_0\epsilon''(\omega)\omega$ is the frequency-dependent relaxation conductivity of bound charge (displacement current). In the limit of high frequency

$$\sigma' \equiv \sigma_\infty = \sigma_0 + \Delta\sigma_D \quad (3)$$

where

$$\Delta\sigma_D = \epsilon_0\Delta\epsilon\tau_D^{-1} \quad (4)$$

is the dielectric conductivity expressed in terms of the polarization strength, $\Delta\epsilon$, and the time constant, τ_D , of the relaxation spectrum.

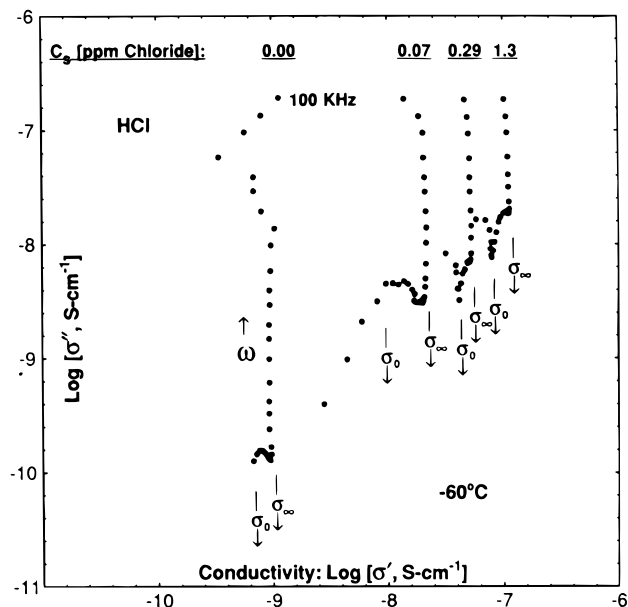


Figure 2. Complex conductivity plots for ice samples doped with HCl. Undoped ice is shown for comparison. Frequency (1 Hz to 100 kHz) is increasing in the direction of the arrow. For other symbols see text. Some low-frequency points have been omitted for clarity (see Table 1 for numerical values).

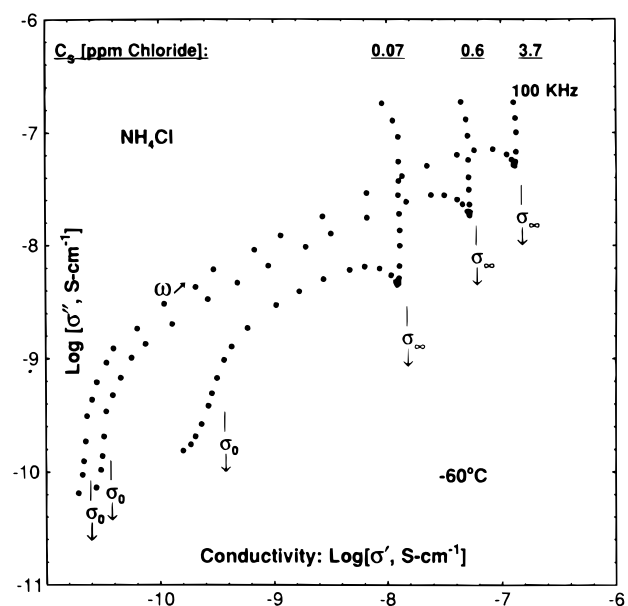


Figure 3. Complex conductivity plots for ice samples doped with NH₄Cl. For explanation see Figure 2 and text (Table 1 for numerical values).

In the bilogarithmic representation of complex conductivity plots the limiting conductivity values, σ_0 and σ_∞ , are ideally given by the abscissa intercepts of vertical plot segments. Departures from verticality in our plots (Figures 2 and 3) are attributed, at low frequencies, to hindered space-charge diffusion and/or stray admittance in the sample cell and, in the high-frequency limit, to response limitations of the lock-in amplifier. In the HCl-doped samples (Table 1 and Figure 2) σ_0 increases with solute content, and the dielectric conductivity is of comparable magnitude. In NH₄Cl-doped samples (Figure 3), by contrast, σ_0 decreases with solute concentration while $\Delta\sigma_D$ increases and is larger by orders of magnitude. This increase is linked to a large reduction of the dielectric relaxation time (eq 4). Similar response has been observed for other ammonium salts, notably the fluoride,^{1,13} the sulfate,¹⁴ and the nitrate (Table 1).

Discussion

A. Defect Mechanisms in Ice. Solute interaction with the ice lattice generates *extrinsic* orientational (Bjerrum) and ionic point defects.⁴ In an electric field, positive ion defects (H_3O^+) transport net charge through the sample, giving rise to σ_0 . At constant temperature, σ_0 is proportional to a fractional power of solute concentration (ref 4, Figure 12). This effect is dominant with acid solutes, such as HCl. Orientational defects control the relaxation of water dipoles (bound charge), τ_D , and $\Delta\sigma_D$ (eq 3). This effect is dominant with NH_4Cl .

B. Where Are Solutes Located in the Ice Matrix? High solubility of ammonium fluoride in ice can plausibly be attributed to substitution of two water molecules by one NH_4F . This is explained by similarities between these two species:^{1,15,16} they are crystallographical isomorphs; both groups, O—O and N—F, have the same number of outer-shell electrons; both molecules have polar groups; the ratios $\text{H}/(\text{N} + \text{F})$ and $\text{H}/(\text{O} + \text{O})$, respectively, are the same for both molecules, enabling them to form the same number of hydrogen bonds required for the undisturbed ice structure. It is less plausible, however, to make the substitution argument for other anions, bicarbonate, sulfate, nitrate, or even chloride, which is the halide next in size above the fluoride. Yet in comparison with their acids or alkali-metal salts, these large anion species also show a higher solubility in ice when associated with ammonium, although none of them comes close to the solubility of the ammonium fluoride in ice (compare values of k_x in Table 1).

We propose that ammonium, by virtue of its structural similarity to the water molecule (ref 16, p 54), especially its polar moment together with its unusual ability to donate and accept hydrogen bonds,¹⁷ facilitates the *coupling* of anions (of any size) to the ice lattice, whereupon they can be incorporated into the solid matrix and accommodated in "microstructures",¹⁸ microfractures,¹⁹ dislocations,²⁰ especially electrically charged ones,^{19,21} interstitials,²² "vested" vacancies (those with dangling bonds),²² and grain boundaries.²³ To understand and model the dynamics of chemical adsorption processes at the ice surface and their role in bulk phenomena, such as those reported in this paper, we need to learn where these species are located in relation to the ice lattice and to its inhomogeneities.

Implications for Atmospheric Processes. The presence of NH_4I traces substantially improves the ice-nucleating efficiency of an AgI substrate.²⁴ Thus, ammonium compounds may stimulate the heterogeneous nucleation of ice particles in clouds.

Ice nucleation temperature was raised by as much as 6 °C on a substrate of layered hydrophobic α -amino acid crystals exhibiting a polar axis, as contrasted with nonpolar crystals of identical composition,¹⁹ although structural properties and lattice constants do not match those of ice in either case. The effect has been attributed to a strong electric field generated within submicroscopic cracks oriented normally to the dipole moment and the layering.

Certain thunderstorm electrification theories postulate the role of cloud ice particles in the separation, storage, and eventual discharge of electrical energy either by collision or induction processes. The proposed electrical (and electromagnetic) mechanisms depend on properties greatly affected by solute impurities, such as relaxation times and conductivities.²⁵

It has recently been proposed that conversion of HCl into active Cl_2 at the surface of stratospheric ice particles requires, as an essential first step, ionization of the former.²⁶ The results presented in this paper suggest that this step might be suppressed or at least reduced in the presence of ammonia (and abundant water molecules). An electrical potential develops at an ice/

water interface during nonequilibrium freezing. In the presence of aerosols (SO_2 , NO_2 , HCl) redox reactions and uptake of the gaseous species occur.²⁷ For the two species first named, the reactions appear to be especially effective in the presence of NH_4^+ ²⁸ because the ice acquires a positive charge.²

Acknowledgment. We thank Susan Schima and Raquel Tun for their painstaking laboratory work and data analysis. This research was supported by National Science Foundation Grant ATM 89-21289.

References and Notes

- (1) Brill, R.; Zaromb, S. *Nature* **1954**, *173*, 316. Zaromb, S.; Brill, R. *J. Chem. Phys.* **1956**, *24*, 895.
- (2) Workman, E. J.; Reynolds, S. E. *Phys. Rev.* **1950**, *78*, 254. Cobb, A. W.; Gross, G. W. *J. Electrochem. Soc.* **1969**, *116*, 796. Gross, G. W. *J. Atmos. Sci.* **1971**, *28*, 1005. Ammonium is preferentially accepted into the ice matrix over chloride and over all other anions mentioned in this paper except the fluoride. This accounts for the ice-positive freezing potentials, which may exceed 100 V during nonequilibrium freezing.
- (3) Whung, P.-Y.; Saltzman, E. S.; Gross, G. W. *Antarct. J.* **1994**, *29*, 73.
- (4) Gross, G. W.; Wong, P.-M.; Humes, K. *J. Chem. Phys.* **1977**, *67*, 5264.
- (5) Tiller, A. W. *Science* **1964**, *146*, 871.
- (6) Mounier, S.; Sixou, P. In *Physics of Ice*; Riehl, N., Bullemer, B., Engelhardt, H., Eds.; Plenum: New York, 1969; pp 562–570.
- (7) v. Hippel, A. R. *Dielectrics and Waves*; Wiley: New York, 1954; Chapter II-32.
- (8) Gross, G. W.; McGehee, R. M. *IEEE Trans. Electr. Insul.* **1988**, *23*, 387.
- (9) Gross, G. W.; Gutjahr, A.; Caylor, K. *J. Phys.* **1987**, *48*, C1-527.
- (10) The slope of the HCl distribution curve in Figure 1 should equal unity, but it is smaller presumably because of an inhomogeneity in the solute (and/or heat) diffusion field near the interface, which develops as freezing progresses, cf. ref 4 and Figures 8–10.
- (11) Grant, F. A. *J. Appl. Phys.* **1958**, *29*, 76.
- (12) The temperature -60 ± 1 °C was chosen because (a) the extrinsic (impurity) effect dominates the response and (b) the whole relaxation is still within the frequency window of our instrument.
- (13) Brill, R. Structure of Ice. Siple Report 33; U.S. Army Snow Ice and Permafrost Research Establishment (Corps of Engineers), July 1957, p 37. Gross, G. W.; Wu, Chen-ho; Bryant, L.; McKee, Ch. *J. Chem. Phys.* **1975**, *62*, 3085. Gross, G. W.; Cox Hayslip, I.; Hoy, R. N. *J. Glaciol.* **1978**, *21*, 143 (see Figure 10).
- (14) Gross, G. W.; Whung, P.-Y.; Saltzman, E. S. *EOS, Suppl.* **1993**, *74* (43), 175 (abstract A51F-II). Gross, G. W.; Svec, R. K.; Whung, P.-Y. *Antarct. J.* **1994**, *29*, 75.
- (15) Pauling, L. *The Nature of the Chemical Bond*, 3rd ed.; Cornell University Press: Ithaca, NY, 1960; Chapter 12.
- (16) Kavanau, J. L. *Water and Solute-Water Interactions*; Holden-Day: San Francisco, 1964.
- (17) Perrin, C. L.; Gipe, R. K. *Science* **1987**, *238*, 1393.
- (18) Truby, F. K. *J. Appl. Phys.* **1955**, *26*, 1416. Gentile, A. L.; Drost-Hansen, W. *Naturwissenschaften* **1956**, *43*, 274. Drost-Hansen, W. *J. Colloid Interface Sci.* **1967**, *25*, 131. Bilgram, J. H. *Phys. Condens. Mater.* **1970**, *10*, 317.
- (19) McBride, J. M. *Science* **1992**, *256*, 814. Gavish, M.; Wang, J.-L.; Eisenstein, M.; Lahav, M.; Leiserowitz, L. *Science* **1992**, *256*, 815.
- (20) Sherwood, C.; Whitworth, R. W. *Philos. Mag. A*, **1992**, *65*, 85. The authors note that HCl doping had no effect on dislocation velocity.
- (21) Itagaki, K. *Adv. X-Ray Anal.* **1970**, *13*, 526.
- (22) Bilgram, J. H.; Roos, J.; Gränicher, H. Z. *Phys.* **1976**, *B23*, 1.
- (23) Petrenko, V. F.; Whitworth, R. W. *CRREL Special Rep.* **1994**, *94* (12), 19. Prodi, F.; Nagamoto, C. T. *J. Glaciol.* **1971**, *10*, 299. Wolff, E. W.; Paren, J. G. *J. Geophys. Res.* **1984**, *89B* (11), 9433. Mulvaney, R.; Wolff, E. W.; Oates, K. *Nature* **1988**, *331*, 247.
- (24) Blair, D. N.; Davis, B. L.; Dennis, A. S. *J. Appl. Meteorol.* **1973**, *12*, 1012. Davis, B. L.; Johnson, L. R.; Moeng, F. J. *J. Appl. Meteorol.* **1975**, *14*, 891.
- (25) Gross, G. W. *J. Geophys. Res.* **1982**, *87C* (9), 7170.
- (26) Clary, D. C. *Science* **1996**, *271*, 1509. Gertner, B. J.; Hynes, J. T. *Science* **1996**, *271*, 1563.
- (27) Finnegan, W. G.; Pitter, R. L.; Young, L. G. *Atmos. Environ.* **1991**, *25A*, 2531.
- (28) Iribarne, J. V.; Barrie, L. A. *J. Atmos. Chem.* **1995**, *21*, 97. Takenaka, N.; Ueda, A.; Daimon, T.; Bandow, H.; Dohmaru, T.; Maeda, Y. *J. Phys. Chem.* **1996**, *100*, 13874.